Spectrochimica Acta Part A: Molecular and Biomolecular Spectroscopy 251 (2021) 119410

Contents lists available at ScienceDirect

Spectrochimica Acta Part A: Molecular and Biomolecular Spectroscopy

journal homepage: www.elsevier.com/locate/saa

Intracellular pH – Advantages and pitfalls of surface-enhanced Raman scattering and fluorescence microscopy – A review

Aleksandra Jaworska [a,*], Kamilla Malek [b], Andrzej Kudelski [a,*]

[a] Faculty of Chemistry, University of Warsaw, 1 Pasteur St., 02-093 Warsaw, Poland
[b] Faculty of Chemistry, Jagiellonian University, Gronostajowa 2, 30-387 Krakow, Poland

HIGHLIGHTS

- Intracellular pH measurements using SERS and fluorescence are described.
- The motivations to carry out intracellular pH measurements are briefly discussed.
- Determination of the intracellular pH plays important role in early diagnostics.

GRAPHICAL ABSTRACT

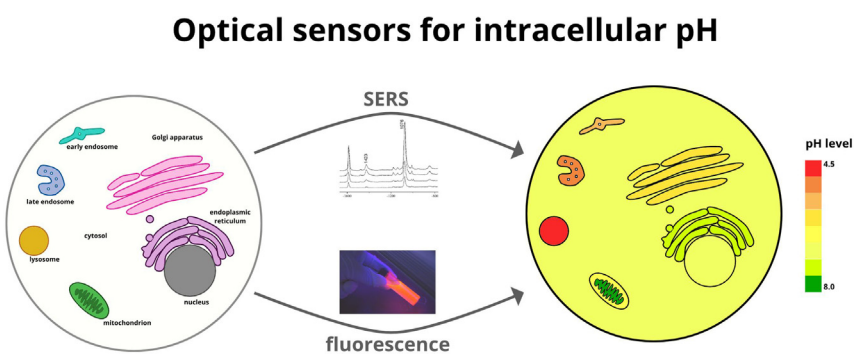

ARTICLE INFO

Article history:
Received 28 September 2020
Received in revised form 19 November 2020
Accepted 29 December 2020
Available online 31 December 2020

Keywords:
Intracellular pH
SERS microscopy
Fluorescence microscopy
Cells

ABSTRACT

The value of pH in various parts of protoplasm can affect nearly all aspects of cell functions. Therefore, the determination of intracellular acid-base features is required in many areas of biological and biochemical studies. Because of a significant scientific importance of *in vivo* intracellular pH measurements, various groups carried out such experiments. In this review article we describe intracellular pH measurements using two the most sensitive optical spectroscopies: surface-enhanced Raman scattering (SERS) and fluorescence. It is reasonable to present these two techniques in one review article because the experimental approach in Raman and fluorescence experiments is relatively similar. The basic theoretical background explaining the mechanism of operation of fluorescence and SERS sensors are discussed and the motivations to carry out intracellular pH measurements are briefly described. Future perspectives in this field are also discussed.

1. Introduction

Local detection of various species in cells is important in order to understand the mechanism of their activity. Therefore, precise methods of quantification of different compounds in biological samples from large complex organic molecules (e.g. various enzymes, DNA) to simple inorganic ions (e.g. Na^+, K^+, Ca^{2+} or Cl^-) are needed. This obviously facilitates understanding of biological and dysfunctional processes and, in the next step, allows constructing a new tool for the clinical diagnosis. Among other ions, the detection and quantification of hydrogen cations in living cells is of particular interest, because of their vital role in physiological and pathological processes as well as the fact that changes in their concentration directly affect the normal body and physiological functions [1] (see Table 1).

* Corresponding authors.
E-mail addresses: ajaworska@chem.uw.edu.pl (A. Jaworska), akudel@chem.uw.edu.pl (A. Kudelski).

https://doi.org/10.1016/j.saa.2020.119410
1386-1425/

Table 1
Comparison of the most important factors for the pH_i measurements using fluorescence and SERS.

	Fluorescence	SERS
Reproducibility of the sensor	High	Sometimes low due to the uncontrollable aggregation of plasmonic nanostructures that form the SERS nanoresonator
Simplicity of data analysis	Similar	
Experimental procedure for the organelle targeting experiments	Similar	
Costs	Similar cost of apparatus; Higher cost of SERS nanoprobes	
Resolution of pH_i mapping	Similar spatial resolution; Better spectral resolution	
Limit of detection	Similar	
Multiplexing	Significantly restricted	Possibility of large level of multiplexing

In this article, we summarize the latest development of the design and applications of various *in vitro* intracellular pH (pH_i) sensors utilizing two the most sensitive spectroscopic detection systems based on surface-enhanced Raman scattering (SERS) and fluorescence (FL) phenomena. Since the experimental approach in SERS and fluorescence experiments is relatively similar, it is reasonable to present the two techniques in terms of their pH labels, technical operation, advantages as well as shortcomings. Motivations of intracellular pH measurements are also briefly described and physical background explaining the mechanism of fluorescence and SERS pH sensing is presented. In principle, the SERS and FL-based pH_i determination relies on measurements of changes in the corresponding spectra of so-called pH sensor which is a chemical compound sensitive to pH alternation of the surrounding environment, on the contrary to the direct determination of many other compounds in cells, where the detection is usually based on the measurement of various types of spectra characteristic for the analyzed compound. The fundamental aspect is the choice of the proper pH_i indicators which will response to acidity of the intracellular environment and give SERS and FL and from this reason it is needed to review molecules required to construct SERS and fluorescence sensors. At the end of this article future perspectives in the field of optical *in vivo* intracellular pH sensors are presented. We hope that this review will encourage more groups of researchers to take up this fascinating topic and make it easier for the new groups to start working in this field of research.

2. Intracellular pH and its significance for the recognition of cellular dysfunction

Hydrogen ions in cellular compartments come from numerous biochemical substances and water ionization [2]. The concentration of H^+ ions can affect nearly all aspects of cell function, e.g. cell metabolism (pH variation can induce changes in the shape of active sites in enzymes or even denature them), cross-linking and polymerization of cytoskeletal elements such as actin and tubulin, proliferation, migration, ability of muscle cells to generate tension or the work of ion-selective channels [3]. The pH value in different cellular compartments, body fluids and organs is usually tightly regulated in a process called acid–base homeostasis [1]. Cellular organelles like nucleus, mitochondria, lysosomes, endoplasmic reticulum (ER), Golgi apparatus, lipid droplets and so on, play important roles in ensuring the smooth progress of cell growth, proliferation, fission, signal transduction and apoptosis by maintaining subcellular microenvironments [4]. They are also the main sources as well as targets of diverse bioactive species. So, abnormal pH values in cells and tissues largely influence the normal functions and activities of body, associated with serious diseases such as cancer and Alzheimer's disease [2,6–9].

Protoplasm participates in many important physiological and pathological processes regulating cellular biological functions [2,86–88]. The dysfunction of organelles leads to a variety of aberrant regulations and multiple diseases such as lysosomal storage diseases, neurodegenerative diseases, neuromuscular disorders, infectious diseases, auto-immune diseases, glycosylation diseases, and cancer. Cellular organelles independently control their internal pH. For example, mitochondrial pH is higher than in cytoplasm (~8.0 in matrix, ~7.1 in the intermembrane space, IMS) whereas lysosomes and endosomes are more acidic, i.e. their acidity is in the range of 4.5–5.0 and 5.4–6.4, respectively. Moreover, a decrease of lysosomal pH is observed in cancer cells in contrary to the overall change of pH of the whole cell [89]. But not only pH of cellular organelles can change independently but also cytosolic pH_i varies in distinct parts of the cell. In general, pH of the cytoplasm is 7.2 and it is critical to maintain this value for any given organism [90]. Phosphate, bicarbonate ions and weak acids and bases present in the cell mainly provide the intracellular buffering capacity. Side-chains, free amino and carboxy-termini of amino acids, and proteins contribute to that less than 1%. Indeed, only histidine (pK_a ~6.04) and other imidazoles affect buffering near neutral pH. For example, approximate pH values of HeLa cytoplasm, mitochondria, endoplasmic reticulum, and Golgi apparatus were determined to be 7.4, 8.0, 7.5, and 6.6, respectively. For comparison, the pH values of various eukaryotic compartments and organelles were reported to be 7.2 for the cytosol, nucleus (due to membrane permeability) and endoplasmic reticulum, 6.7 and 6.0 for cis- and *trans*-Golgi cisterns, respectively, 8.0 in mitochondria, 7.0 in peroxisomes, 5.5 in secretory granules, 6.3 in early endosomes, 6.5 in recycling endosomes, 5.5 in late endosomes, and 4.7 in lysosomes. A schematic of the averaged pH values for cellular organelles is shown in Fig. 1 [60,91].

One of the most-known examples of alterations in the intracellular pH is tumorigenesis [2,6,9]. Tumor microenvironment is characterized by slightly acidic values outside the cells (pH around 6.5–

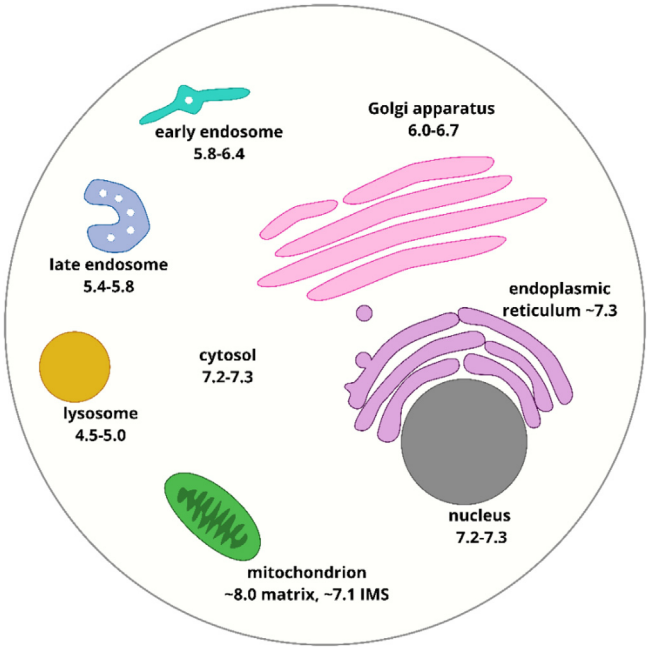

Fig. 1. pH of the different subcellular compartments from ref. [60,91].

7.0) and slightly alkaline intracellular pH (*ca.* 7.2–7.4, see Fig. 2) [6]. These properties of cancer cells are used in the oncologic treatment by a design of nanomaterials targeting the specific pH regions in cells, e.g., in photodynamic therapy. Also, as acidification of cellular endosomes and lysosomes is crucial for the correct trafficking of these organelles, the inhibition of this process induces apoptosis of tumor cells, therefore specific inhibitors of proton ATPases can be used as anticancer therapeutics [10]. Changes in the pH_i will also influence the activity of enzymes by affecting the ionization state of acidic or basic amino acid residues, which may disrupt ionic bonds determining the 3-dimensional shape of the enzyme. These conformational alterations can lead to inactivity of the enzyme due to restricted binding of substrates or cofactors. In addition, the modification of intracellular pH can change the charge properties of the substrate, so that either the substrate cannot bind to the active site or it cannot undergo catalysis [10]. In turn nervous system diseases such as ischemic stroke, traumatic brain injury, epilepsy, Parkinson's disease, and Alzheimer's disease (AD) show the decreased pH or acidosis at both tissular and cellular levels. Particularly, some AD-associated enzymes exhibit altered activity under acidic conditions [7]. The exact pH_i in AD neurons has not been yet determined, but, as shown for brain ischemia, pH_i falls down below 6.5 quenching neuronal activity and inducing cell apoptosis, amyloid plaques deposition, tau phosphorylation as well as inactivation of AD-associated enzymes [8].

These few examples highlight the need of monitoring the intracellular pH, as its changes, although very subtle sometimes, appear in dysfunctional organelles, cells or their colonies. Nowadays there are few methods which are employed for this purpose [92], including H^+ permeable (glass) microelectrodes, emission/excitation of weak acid fluorescent dyes, nuclear magnetic resonance (NMR) analysis of metabolites whose resonance frequency is influenced by pH. Recently, surface-enhanced Raman spectroscopy (SERS) has been developed for this purpose and can be a good alternative for routinely used methods [60]. To monitor pH in specific organelles, fluorescence-based detection is the most common technique due to its simplicity and high sensitivity, but SERS sensors are also established toward this targeting.

3. Monitoring intracellular pH with the use of fluorescence and SERS detection

Both fluorescence- and SERS-based pH sensors act through the generation of light due to emission and scattering phenomena, respectively. Briefly, pH-sensitive fluorescent probes are fluorescent dyes or their conjugates with quantum dots, carbon or polymer-based nanoparticles whereas SERS probes consist of Au and Ag nanoparticles functionalized with an organic molecule with a high cross-section for Raman scattering (Raman reporter). The dye and Raman reporter possess functional groups whose spectral properties change due to pH alternation. Then, they are introduced into cells usually by the endocytic uptake or with the help of cell-penetrating peptides (CPPs, short peptides with 30 or less amino acids) having membrane transduction abilities [11]. The incubation process needs to be optimized to the type of a cell and targeting organelles. Next, FL and SERS signal from cell cultures is collected with the use of the corresponding microscopies. The determination of pH values requires calibration curves showing the relationship between the signal and pH. Some sensors will be described with more details in the two following sections.

3.1. Fluorescence

The ability of specific dyes to change their color in response to a pH change has found widespread application in research and industry [12]. Fluorescent dyes provide a sufficient sensitivity required for optical pH measurements inside live cells together with high ion selectivity which reduces background signal. In addition, the fluorescence microscope rapidly and simultaneously collects the signal from tens of cells and provides a better spatial sampling capability than microelectrode techniques. The pH inside a cell varies by only fractions of a pH unit and any changes can be so small that dyes must be carefully selected regarding their pK_a. Therefore, FL pH indicators act selectively in acidic environment (for lysosomal and endosomal pH) and nearly neutral pH (for cytoplasm, mitochondria and nuclei). One of the most popular dyes are litmus, phenolphthalein, phenol red and their derivatives.

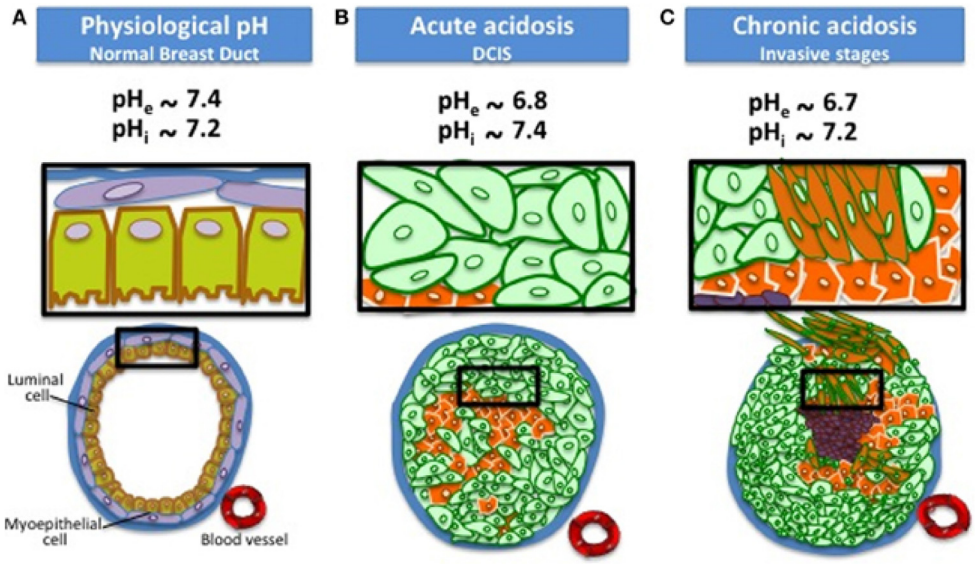

Fig. 2. Reversed extracellular and intracellular pH in cancer cells compared to normal cells. Cancer cells have a reversed pH gradient compared with normal differentiated cells that is, cancer cells have a higher pH_i and a lower pH_e than normal cells in acute acidosis conditions. The pH_e becomes even lower (~6.7) in chronic acidosis. Reprinted from ref. [6] under the terms of the Creative Commons Attribution License (CC BY). Copyright © 2013 Damaghi, Wojtkowiak and Gillies.

The experimental procedure for fluorescence measurements of pH_i is very simple, i.e. cells are loaded with a fluorescent probe, whose fluorescence signal varies with pH. Usually, dyes are in a form of acetoxymethyl ester (AM), which is readily permeable to cell membranes. Esterification with AM groups converts negatively charged membrane-impermeant acids into neutral, membrane-permeant ester analogues [13]. A drawback of such a modification of the dyes is a decrease of their water solubility, so the use of surfactants is often needed [14]. Once inside the cell, the AM groups are cleaved by ubiquitous intracellular esterases, which release charged species that cannot exit the cell. In recent years, many review articles summarizing recent developments and achievements in the field of the pH-sensitive fluorescence sensors have been published [1,4,15-27]. However, only few are commercially available, suggesting that there are still some major problems to solve, e.g., low quantum yield, photodegradation due to long-term exposure time, low signal-to-noise ratio due to interference from non-specific binding, autofluorescence or lack of sufficient selectivity [28].

Additionally, pH indicators can be delivered to specific cellular compartments either by conjugation to targeting molecules or by partitioning into more acidic compartments by protonation. Various LysoSensorTM probes are synthesized in that way as summarized on a Thermo Fisher website [93]. These probes reach the lysosomes because of the presence of typical lysosome-targeting moiety of morpholine in their structure [94]. Also, pH-sensitive green fluorescent proteins (GFPs) variants that are sensitive to pH changes allow precise compartmental targeting via fusion proteins partitioning into more acidic compartments by protonation. After being loaded into cells, fluorescent molecules absorb photons of light of the appropriate excitation wavelength and then energy is emitted at a longer wavelength (emission wavelength) than for excitation, e.g., for LysoSensor™ Blue Excitation/Emission is 373/425 nm, for LysoSensor™ Yellow/Blue: 329/440 or 335/452 nm, for LysoSensor™ Green 443/505 nm. In Fig. 3, there is an example of commercially available LysoSensor Green: the structure and fluorescence images in aqueous solution at different pH (Fig. 3A) and relative fluorescence intensity as a function of pH (Fig. 3C, blue curve) [29].

Unfortunately, most commercially available sensors are just pH sensitive without the possibility of organelle-targeting and thus they label any acidic vesicle, making the reagents "selective" rather than "specific" [30]. Moreover, manufacturer specifications lack detailed information on calibration curves and errors and therefore it is difficult to judge how reliable is the pH readout below 0.1 unit (as in majority of publications the calculated/measured/estimated pH value is given to two decimal places).

A very interesting approach to pH_i measurements is an "on–off" system instead of the continuous change of the fluorescence intensity [29,31]. X. Ma et al. developed ultra-pH sensitive (UPS) copolymers with sharp pH transitions that are finely tunable in a broad range of physiological pH [31], justifying this approach that the continuous change of fluorescence intensity hampers its ability to differentiate small pH variations between pathological pH (e.g., acidic tumour pH, 6.5–6.9, and normal pH ~ 7.4) [29]. These UPS nanoparticles consist of amphiphilic block copolymers (see Fig. 3b), where PEO is poly(ethylene oxide) and PR is hydrophobic block with multiple ionizable tertiary amines. At low pH, micelles dissociate into cationic unimers with protonated ammonium groups (see Fig. 3d). When pH increases, neutralized PR segments become hydrophobic and self-assemble into core–shell micelles. This strategy was successfully employed for measurements of many biological systems, e.g., differentiation between endosomes and lysosomes [26].

Also, an interesting approach was shown by Wang et al., where Janus nanoparticles were modified with 2 different fluorescent dyes: rhodamine B and fluorescein isothiocyanate [32]. This approach improved the calibration curve (ratio of 2 different molecules' signal instead of 1) providing more precise pH values and an excellent linear relationship in the physiologically relevant pH range of 4.0–6.0.

Apart from targeting cytoplasm and lysosomes, more and more attempts are made to perform measurements in other organelles, for example mitochondria [33,34]. H. Huang et al. developed a fluorescent nanosensor for simultaneous detection and imaging of pH and $O_2^{\bullet-}$ species in mitochondria of live RAW264.7 macrophage cells [33]. CdSe/ZnS quantum dots were encapsulated in a silica shell and functionalized with a mitochondria-targeted molecule (4-carboxybutyl)triphenylphosphonium bromide (TPP) and a pH-sensitive fluorescent dye fluorescein isothiocyanate (FITC). Mitochondrial pH was recorded between 5.9 and 7.9.

Despite above-mentioned advantages of FL-based pH sensors, this method has also some disadvantages making the determination of intracellular pH_i demanding. First of all, photobleaching of fluorescence features of dyes does not allow for a prolonged exposure of the samples to excitation light and requires careful operation of the samples. In-activated FL-based pH sensors disturbs the quantification of FL intensity and in consequence can provide to false conclusions. Moreover, fluorescence of the pH-sensitive dye may suffer from interference of an endogenous biological molecule-triggered background signal and makes multiplex targeting of few organelles very difficult. Since pH indicator is localized only in some cellular structures, other cellular compartments are not visualized and to do it other staining is required but the incubation of cells with other FL labels can affect the pH. It might also happen that theoretically pH-sensitive dyes become indifferent to intracellular pH changes, but may indicate fluorescence activation by membrane structures [17]. Therefore, this needs to be carefully tested when introduced into intracellular environment. Another problem occurring is poor water solubility of some dyes (e.g., SNARF derivatives), which makes it difficult to implement for intracellular sensing of pH in a reliable and convenient way [35] while enhancing of FL signal by the use of quantum dots is limited due to their high cytotoxicity.

Even though fluorescence microscopy is the fundamental technique in many *in vitro* laboratories, its use for this particular purpose is still limited due to mentioned shortcomings. It has been already shown that this technique can be complemented by surface-enhanced Raman spectroscopy (SERS). There are several reports that have proven a similar effectiveness of SERS and FL or attempts to design dual-signal sensors [36,37]. Due to (1) ultra-high detection sensitivity up to the single-molecule level, (2) narrow and sharp spectral peaks for multiplex detection, and (3) the lack of interference in diverse environments, such as oxygen, humidity, and foreign species, SERS has become increasingly attractive for the detection of biological species in living cells and tissues. In the next chapter, the brief overview of the SERS intercellular pH sensors is given.

3.2. Surface enhanced Raman scattering (SERS)

Raman spectroscopy is a method that enables vibrational modes of individual bonds to be probed optically and has been widely employed in various biomedical experiments. While Raman scattering is a weak effect, for molecules adsorbed on nanostructured metal surfaces of silver and gold the efficiency of the generation of Raman signal can be enhanced by up to 14 orders of magnitude by means of surface-enhanced Raman scattering (SERS) [38]. The increase in the efficiency of the generation of the Raman signal in the SERS effect is mainly caused by the increase in the intensity of the electric field in the close proximity to the illuminated plasmonic nanostructures (as nanostructured gold and sil-

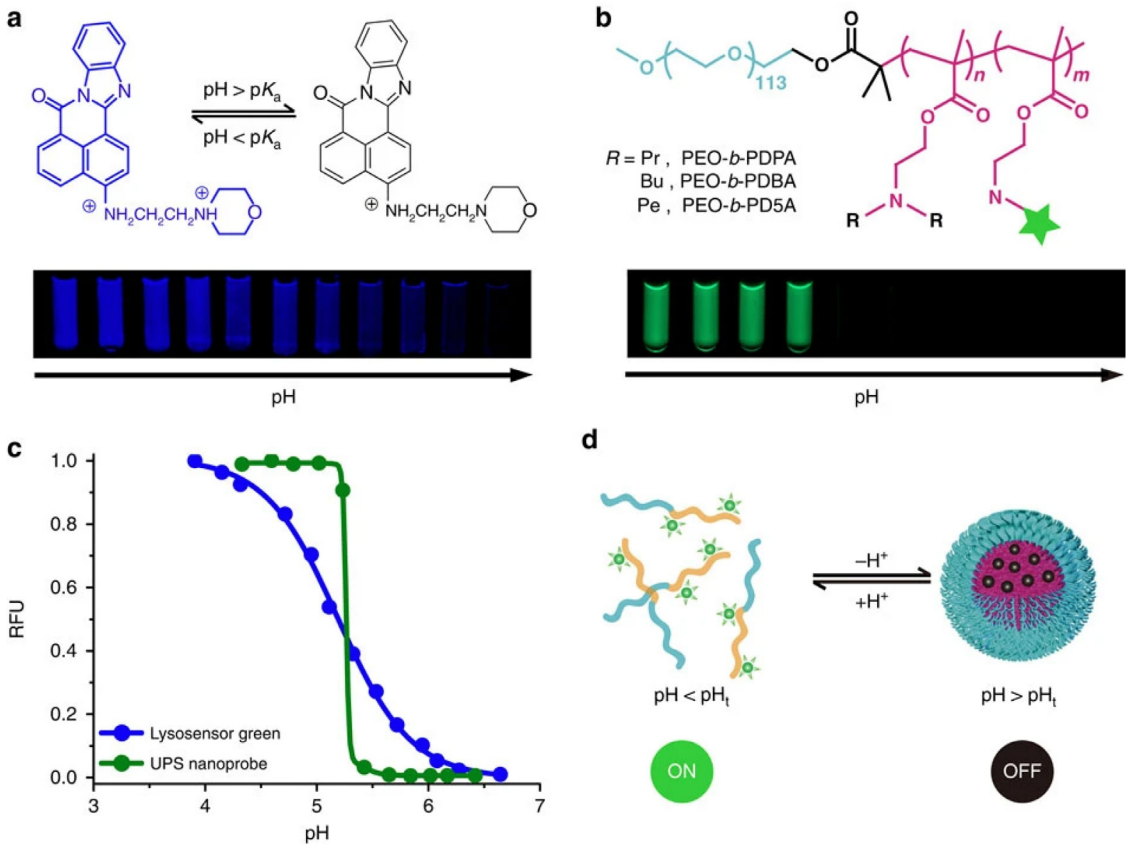

Fig. 3. (a) Structure and fluorescence images of a small molecular pH sensor, Lysosensor Green in aqueous solution at different pH. (b) Structure and fluorescence images of a ultra-pH sensitive (UPS) nanoprobe, Rhodamine Green-conjugated PEO-b-PDBA block copolymers in aqueous solution at different pH. (c) Relative fluorescence intensity as a function of pH for Lysosensor Green and PEO-b-PDBA-RhoG nanoprobe. (d) Schematic illustration of pH-triggered binary on/off transition of UPS nanoprobes. Reprinted from ref. [29]. The figure is from an open access article distributed under the terms of the Creative Commons CC BY license. Copyright © 2016, Springer Nature.

ver). When nanoparticles formed from plasmonic metals (in general, metals with a negative real and small positive imaginary dielectric constant at the frequency of the illuminating radiation) are irradiated by the radiation having the proper frequency, the electric field of the electromagnetic wave induces collective oscillations of surface conduction electrons, called surface plasmons, which can be treated as oscillating electric dipoles generating additional electric field in a close proximity of the illuminated nanoparticle. For example, for a spherical metal nanoparticle, the magnitude of the induced dipole (p) is proportional to [39]:

$$p \; \frac{\epsilon_M(\nu) - \epsilon_{out}(\nu)}{\epsilon_M(\nu) + 2\epsilon_{out}(\nu)}$$

where: ν is the frequency of the used excitation radiation, $\epsilon_M(\nu)$ and $\epsilon_{out}(\nu)$ are the dielectric functions of the metal and the surrounding medium, respectively. When the denominator of this fraction is close to zero, the strong electric dipole is induced, which leads to a large local intensity of the electric field. It happens, when the value of $\epsilon_M(\nu)$ is close to the value of $-2\epsilon_{out}(\nu)$. The dielectric function of the metal [$\epsilon_M(\nu)$] is a complex number, and hence, to better satisfy in full the condition $\epsilon_M(\nu) = -2\epsilon_{out}(\nu)$, which would imply $p \to \infty$, also the imaginary part of Im[$\epsilon_M(\nu)$] at a given ν should be small. This condition may be fulfilled in some regions of the visible radiation for example for gold and silver nanoparticles.

In SERS spectroscopy, the increase in the intensity of the measured Raman signal is roughly proportional to the fourth power of the field enhancement [40,41]. This fourth power dependence of the SERS enhancement factor on the field enhancement often leads to a very large increase in the efficiency of the generation of the measured SERS signal, and, as mentioned in the introduction, in some cases, it is possible to record SERS signal even from a single molecule [42,43]. Moreover, in addition to the electromagnetic enhancement, the efficiency of the generation of SERS spectra is increased due to the so-called chemical enhancement. For adsorbed molecules the mechanism of this enhancement is analogous to the standard resonance Raman process. Briefly, the interaction of adsorbed molecules with the metal substrate provides new electronic transitions for metal (or adsorbed molecule) electrons. The electrons at the Fermi level of the metal can be virtually excited into unoccupied molecular orbitals of adsorbed molecule or the electrons at the highest occupied molecular orbital can be virtually excited into Fermi level of the metal.

Since its discovery, possible applications of SERS spectroscopy are rapidly growing, from physicochemical studies on the interaction of molecules with different metal surfaces (for example determination of: the mechanism of bonding, the orientation of adsorbed molecules versus the metal surface, the changes of the structure of the adsorbed molecules upon interaction with the metal surface) to many analytical applications (especially in environmental analysis and in food quality control) including *in vivo* analysis of complex biological samples with trace amount of searched compound. Medical applications have been especially widely developed because of ultra-low limit of detection (up to single molecule level), impossible to achieve by many different analytical methods [38,44-50]. Probes used for SERS experiments can be stable even for couple of months and with appropriate design they are non-cytotoxic, in particular when Au nanoparticles

are the core of the nanosensor. Also, each molecule features different SERS spectrum connected to its structure, so with careful selection of probes when bands do not overlap multiplexing is possible at very high level [51-54]. To push SERS towards clinical applications, cells and tissues are being of interest as a research topic. Especially in the case of cells, an enormous progress has been made in experimental approach [54,55].

The first SERS-based cellular studies were performed by addition of nanoparticles or nanoparticles labelled with Raman reporter molecules to cellular medium and recording the signal from the random cellular compartments [55–57] and/or Raman reporter molecules [55,56,58]. That was a big breakthrough, however, the uptake of nanoparticles and their accumulation in cells were not controlled and these experiments showed only the pathway of introduction of nanoparticles inside cells (mainly *via* endocytosis), and that it is possible to obtain SERS spectra from proteins/lipids/DNA present in cells. With this approach, it is possible to monitor intracellular environment with the use of nanoparticles, from their uptake process and then distribution within cells [58] up to biologically important values like pH and redox potential [59,60]

The easiest and earliest approach to monitor pH inside cells by SERS is to add simple nanosensors into cellular medium and let the cells endocyte nanoparticles. These nanosensors consist of pH-sensitive Raman reporter (RR) attached to the surface of plasmonic nanoparticles (Fig. 4A). SERS spectrum of the RR changes as a function of pH (e.g., mercaptobenzoic acid or mercaptopyridine can be used, where carboxylic or amino groups are protonated or deprotonated depending on the pH, and as a result changes in the SERS spectra can be observed). This is called incubation-depletion method, which is simply incubation of the cells in the media containing the nanosensors, washing out not endocyted nanoparticles followed by the incubation in pure media afterwards [61]. Then, SERS measurements are performed and the distribution of nanoparticles is monitored by SERS spectra of Raman reporter molecules, from which local pH inside cell is calculated based on the calibration curve, where the relative intensity of the selected bands is shown as a function of pH. For example, determination of pH using mercaptobenzoic acid as a Raman reporter is made by monitoring the ratio of the intensity of a SERS band at 1430 cm^{-1}, assigned to the vibration of the carboxylate ion (which increases with the increasing pH), to the intensity of a band at 1590 cm^{-1}, assigned to vibration of the aromatic ring (which remains stable in the whole pH range). Kneipp and co-workers introduced small aggregates of gold nanoparticles functionalized with mercaptobenzoic acid to the live fibroblast NIH/3T3 cell and then carried out respective SERS mapping [57]. As a result, they obtained a map of the distribution of H^+ ions (pH) in the living cell divided into regions (see Fig. 5A), where the values of pH were in the range of 6.2 to 7.4 every 0.2/0.3 pH unit [57]. Since 2010, Raman equipment developed with enormous increase in resolution and signal quality, therefore now we are able to obtain much more detailed maps of the distribution of pH within cells (see Fig. 5B) [65]. Mercaptobenzoic acid has been also used for the pH SERS studies of dysfunction of endothelial cells, treated with tumour necrosis factor alpha (TNFα) [60]. It turned out that in these cells the distribution of the nanosensors was more uniformed comparing to the healthy cells, suggesting a disruption of the endocytic pathway leading to nanosensor release into the cytosol or high increase in the formation of endosomes in TNFα – activated cells. Recently, Capocefalo et al. performed detailed study on the stability and reliability of the mercaptobenzoic acid-based nanosensor for pH studies [62]. They employed this nanosensor for pH_i measurements in non-tumorigenic human keratinocyte (HaCaT) and tumorigenic human skin melanoma (SK-Mel5) cell lines, however, the estimated pH was 7.0 ± 0.4, 7.4 ± 0.7 and 6.5 ± 0.9 for HaCaT and 5.6 ± 0.2, 6.3 ± 0.6 and 5.6 ± 0.2 for SK-Mel5 cells, depending on which band in SERS spectra assigned to carboxylic group vibrations was selected for the pH calculation. This shows how the results can vary and indicates that it matters which band is selected for performing the calibration curve. However, this nanosensor was useful for the differentiation between two cell types. Bai et al., in turn, developed nanosensor based on pyridine molecules that turns off when it is outside the cell, thus to be certain that the measured values correspond to the intrinsic pH, not the extracellular environment [63]. In this case, the detected pH was close to neutral (6.0–7.5) in early endosomes and acidic (4.5–6.0) in late endosomes or lysosomes. It turned out, however, that some nanoparticles bound to the cell membrane or adhered to the dish, emitting unwanted SERS signals outside the cells and affecting the pH of the culture medium (detected pH values ~ 7.5).

However, it has been shown recently by Scarpitti et al., that the choice of mathematical approach to the results (e.g. the relative intensity of the ν(COO^-) stretch, chemometric analysis of the ν_{8a} mode, or analyzing the frequency shift of the ν_{8a} mode) influences the calculated pH values [64]. Experiments performed on gold nanoflowers labelled with 4-mercaptobenzoic acid showed different sensitivity to some of these sources of error in live cell experiments. pH determination based on Raman frequency shift appears to give a more reliable pH determination, though in high signal-to-noise environments, intensity ratios may provide better sensitivity to small changes in pH for cellular imaging.

Methodology of preparation of pH-sensitive nanoprobes were developed due to rise their sensitivity and reliability for the biological systems applications. For example, H. Guo et al. amended

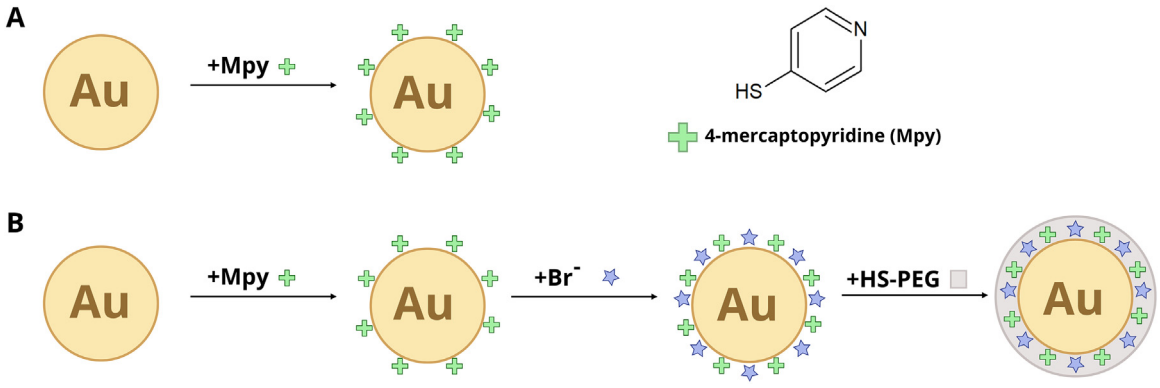

Fig. 4. Schemes of the preparation of the SERS pH-sensitive nanoprobes. (A) The basic version of the sensor, 4-MPy or other pH-sensitive reporter molecules can be used, (B) Scheme of bromide anions and PEG-stabilized sensor, procedure adapted with permission from ref. [64].

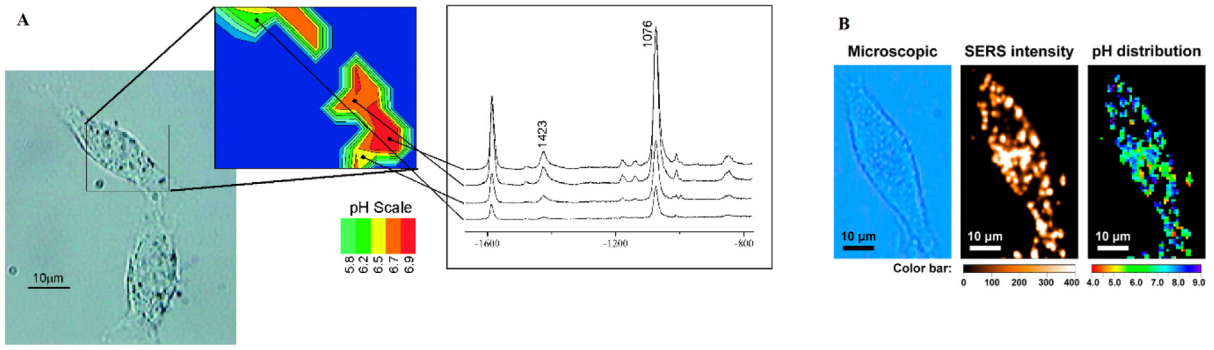

Fig. 5. Probing and imaging pH values in individual live cells using a SERS nanosensor. (A) Photomicrograph of an NIH/3T3 cell after incubation with small aggregates of gold nanoparticles functionalized with 4-mercaptobenzoic acid with pH map and correlating SERS spectra. Adapted with permission from ref. [57]. Copyright (2010) American Chemical Society (B) Microphotography of the human cervical cancer cell together with the distribution of SERS signal and pH map of the cell. Au nanospheres labelled with 4-mercaptopyridine and covered with bovine serum albumin (BSA) as a protective layer were used as nanosensors. Reprinted with permission from ref. [65]. Copyright (2019) American Chemical Society.

4-mercaptopyridine-based nanosensor by using bromide anions [95]. Briefly, 4-mercaptopyridine (4-MPy) was added to the solution of gold nanoparticles labelled with surface ligand ascorbic acid (AA) to replace AA molecules. Then nanoparticles were functionalized with Br^- (Br^- electrostatically stabilizes protonated 4-Mpy, thus enabling sensitive SERS detection of the protonation state of 4-Mpy as a function of pH while also reducing variability caused by external halide ions), and stabilized with HS-PEG as shown in Fig. 4B. These nanoprobes were successfully applied to measure pH in lysosomes of 4 T1 murine mammary carcinoma cells, which ranged from 4.8 to 5.5 (±0.1) within different cells, which is in good agreement with the previous studies.

In a very impressive work by Zhang et al., 3D visualization of endocytic pathway was shown [66]. The use of cationic polymer polyarginine significantly improved stability of nanoprobes and measurements after 8 h since the endocytosis started were possible. The experiment allowed visualization of local changes in pH_i such as acidification during nanoparticle (NP) endocytosis. In another 3D experiment, SERS spectra from the functionalized nano-assemblies which were transported to a cell were recorded to estimate the local pH on the pathways travelled by the nano-assemblies [67]. Bando et al. observed a decrease of pH_i due to the lysosome internalization as well as a decrease in pH around the nano-assembly, which could be induced by a fusion process of lysosome and endosome.

These experiments are relatively easy to perform, however, these nanosensors randomly enter the cell by endocytosis and are trapped in lysosomes, therefore, with this approach we can only measure the lysosomal pH at different stages [63,68-75]. Also, as mentioned above, not all nanosensors are enocyted by cells, therefore some can stick to the cellular membrane, which can lead to false results [63]. Therefore, modifications of the nanosensors should be made. For example, nanosensors can be covered with cell penetrating peptides (CPPs), which enable sensors to target intracellular regions [76]. Nanosensors modified with these peptides enter the cell *via* endocytic pathway, but the process is more effective comparing to the standard sensors' uptake. Also, proteins like bovine serum albumin can be used as a protecting layer [61], additionally they can be marked with a fluorescence dye to track nanoparticles by fluorescence methods [77]. Apart from facilitating the uptake of nanosensors, CPPs help to avoid the situation that majority of nanoparticles are trapped in the lysosomes, and, as a consequence, their distribution within a cell is uneven [78]. These short peptides consisting of *ca.* 5–30 amino acids exhibit low cytotoxicity, however, their first generation can be uptaken only to the intracellular endosomes, thus the presence of additional auxiliary compounds or charged polymers is necessary for their release from these cell organelles, for which these compounds may be toxic. In addition, they can be inactivated by proteases, so if the uptake process last longer (in the case of bigger cargos bound to the peptides), they can be inactivated before reaching the intracellular environment.

Despite these drawbacks, Ma et al. successfully used cell penetrating peptides to monitor the changes of pH induced by hypoxia in tumour cells and tissues [35]. Gold nanorods functionalized with 4-nitrothiophenol (4-NTP) and covered with CPPs (CAAAAAAAK $(ME)_3$, forming biocompatible protective layer and enabling aggregation to increase repeatability of SERS measurements) were used as nanoprobes. Since hypoxia accelerates overexpression of nitroreductase, which catalyzes transformation of 4-NTP into 4-ATP (4-aminothiophenol), SERS spectrum of 4-ATP is pH-dependent. Such an approach allows monitoring pH changes in live adenocarcinomic human alveolar basal epithelial cells (A549) and frozen lung tissue slices. These nanoprobes showed sensitivity to pH changes within 0.5 unit, however study on repeatability of SERS spectra is missing, so it is impossible to compare the efficiency of the methodology with fluorescent studies.

In another study, Zheng et al. used CPPs to study in situ cell cycle in single live human cervical cancer cells (CaSki) [65]. The measurements were performed on a home-built in situ microscopic cell culture platform using Au nanospheres modified with 4-mercaptopyridine (4-MPy) and bovine serum albumin (BSA) as a protective layer. In this case, cysteine-terminated Tat peptide (YGRRRQRRKKRGC) was selected as CPP. This arginine-rich peptide with cationic "character" penetrates the negatively charged plasma membrane directly without the participation of endocytosis and accelerates the cellular internalization process. Tat enables much higher loading density and uniform distribution throughout the whole cell of nanoparticles offering more reliable pH_i distribution estimation, see Fig. 6. This design of pH nanotags showed the differences in the average pH in the cells at the different stages of life cycle. A gradual alkalization from interphase to prophase was observed whereas rapid acidification occurred going from prometaphase to telophase. This process reflected variation and consumption of species related to the energy storage during the cell cycle.

Recently, the construction of SERS pH_i labels were pushed forward targeting mitochondria [79–81] and nucleus [79,80] by attaching organelle-targeting peptides to SERS nanotag in the way similar to the described-above CPPs. According to a report of Shen and co-workers, mitochondria localization peptide with a MLALLGWWWFFSRKKC sentence deliver molecular cargo to the

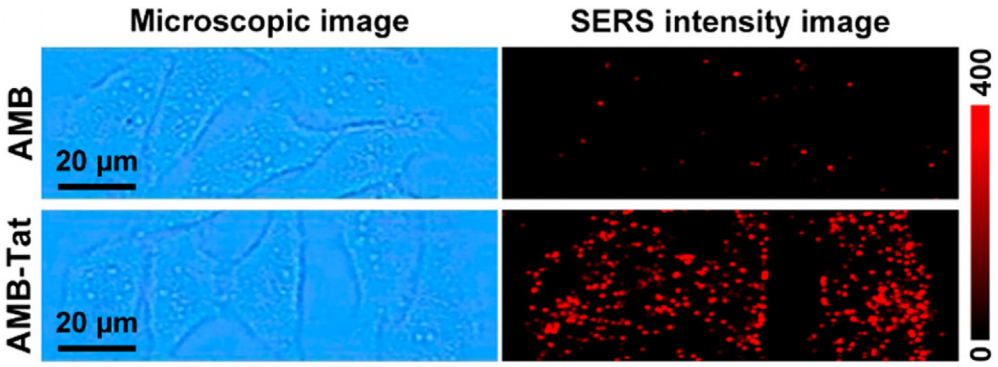

Fig. 6. Comparison of the cellular internalization efficiency of 10 μg/mL nanoprobes without and with Tat peptide. SERS intensity images were produced using the intensities of 1093 cm^{-1} peak. Reprinted with permission from ref. [65]. Copyright (2019) American Chemical Society.

mitochondria by specifically and precisely processing mitochondrial proteases, while nuclear localization peptide (GGVKRKKKPGGC sequence) transports nanoparticles into the nucleus or near the nucleus region due to the characteristic lysine–lysine–lysine–arginine–lysine (KKKRK) sequence [80]. On the other hand Eling et al. noticed that gold nanoparticles simply modified with rhodamine 6F are uploaded to mitochondria [81].

Another way to target specific intracellular parts with SERS nanoprobes is labelling them with specific antibodies targeting appropriate receptors. In that way the FcεRI receptor-mediated endocytic pathway in RBL-2H3 cells was monitored and different stages of endosomal maturation were recognized [82] as well as the temporal and spatial progression of receptors as they traffic through the endosome–lysosome system was followed in bafilomycin or amiloride-treated cells [83].

A very original experimental approach to pH_i measurements is the use of flexible nanopipette [84], a glass capillary loaded with gold nanoparticles labelled with mercaptobenzoic acid. They figured out that the cancerous HeLa cells could effectively regulate their pH_i and better adapt to the weakly acidic extracellular environment than normal cells, such as fibroblast cells.

At the end, it is also effective to combine both SERS and fluorescence due to increase the precision of measurements and extract more information about experimental system. For example, Pallaoro et al., [85], prepared nanosensors consisting of both SERS-active 4-mercaptobenzoic acid and fluorescent HiLyte-555 dye to determine the local pH from the spatially mapped surface-enhanced Raman spectra correlated with the fluorescence, allowing simultaneous single-particle tracking and local pH sensing.

4. Conclusions and perspectives

SERS and fluorescence microscopies are excellent optical imaging tools to determine pH of the intracellular system. While both techniques offer a similar spatial distribution and penetration depth in collection of images of cells, fluorescence microscopy has been already introduced to biomedical laboratories because it is of relatively low cost and good safety profile for *in vitro* research. However, high sensitivity, excellent multiplex capabilities of SERS with the use of a single excitation source, the low background and minimal photobleaching of SERS nanotags lead to significant growth of SERS technologies proposed for cell imaging. Current challenges in the development of both microscopies for the pH_i determination are focused on the synthesis and design of their ratiometric probes in terms of their biocompability and targeting specific organelles in, that the probes preserve their detection capabilities avoiding interferences from microenvironment. The majority of FL dyes are lipophilic structures that can be affected by numerous chemical species in cells and can leak out from cells and organelles. The FL probes work when their large amounts are uploaded to the cells whereas SERS probes deliver the signal at ultralow concentrations. In turn the latter required the construction of metallic nanostructures of well-defined and uniform nanogeometry and the position of the pH-sensitive Raman reporter to achieve highly stable and reproducible signal. Looking at the latest literature reporting the use of these two methods for pH_i measurements we can observe lack of examination of calibration curves for further pH_i calculations – very rarely error bars are included, moreover, the typical pH range is very wide (not occasionally even whole pH range) but every 1 unit. We suggest that we should rather focus on narrower range but with more densely packed points on the curve as well as to select the sensors providing slop of the calibration curve big enough to provide reliable calculations. In the case of fluorescence, "on – off" system is an interesting option provided that we are able to select precisely at which pH value the sensor switches off. In our opinion, so far published data reliably demonstrate the utility of SERS for showing the differences in pH between different cell cultures or the cellular response to some drastic factors like TNFα, buffers with the pH very different to the cellular pH or heating, however, biological pH changes are subtle and require stable metallic nanostructures. To provide that, anisotropic metallic nanostructures like nanostars, nanostrawberries, nanocubes, nanorods and many others should be used, as they were proven to generate single-nanoparticle SERS. Here an extensive collaboration of chemists and biologists is crucial for further developing structure of probes with highly selective and non-toxic properties. Also, we think that it is crucial to compare the results obtained by different independent methodologies to provide reliability of the results. Also, SERS offers multiplexing capabilities much wider than fluorescence, as the latter is limited by the number of different channels in the equipment (right now 5). In the case of SERS measurements, assuming that one can relative easy determine the intensity of "standard" Raman bands separated by 30 cm^{-1}, using a properly selected set of Raman reporters giving characteristic SERS bands in the spectral region between 600 and 1800 cm^{-1} allows to obtain signals in 40 Raman channels, and therefore, allows to monitor pH in more cellular organelles simultaneously. Comparison of the most important factors for the pH_i measurements using fluorescence and SERS is presented in Table 1.

By highlighting the latest and the most representative reports, this review summarized current strategies for the detection of intracellular pH. Translation of SERS technology to biomedical applications is not yet explored. Several papers showed its important advantages. Current efforts should be aimed to consolidate the technology which will allow rapid large-area imaging, extension of

pH-sensitive Raman reporters and synthesis methods to conjugate metal nanoparticles with organelle-targeting molecules. More attention should be also paid to prove highly precise and sensitive read-out of pH values. Furthermore, most SERS pH indicators are simply constructed of bare metallic nanoparticles and Raman reporter what is far from requirements to avoid interference with cellular biomolecules, significant efforts must be made for designing protective matrix and enhancing biocompatible cell entrance of the nanotags.

Declaration of Competing Interest

The authors declare that they have no known competing financial interests or personal relationships that could have appeared to influence the work reported in this paper.

Acknowledgements

A.J. and A.K. thank the Faculty of Chemistry, University of Warsaw for its financial support. K.M. was supported by the National Science Centre (NCN, Poland) – grant UMO-2016/21/B/ST4/02151. AJ thanks M. Sc. Edyta Pyrak from Warsaw University for the help with the preparation of Figures.

References

[1] J. Yin, Y. Hu, J. Yoon, Fluorescent probes and bioimaging: alkali metals, alkaline earth metals and pH, Chem. Soc. Rev. 44 (2015) 4619–4644, https://doi.org/10.1039/C4CS00275J.
[2] P. Swietach, What is pH regulation, and why do cancer cells need it?, Cancer Metastasis Rev. 38 (2019) 5–15, https://doi.org/10.1007/s10555-018-09778-x.
[3] S. Tatapudy, F. Aloisio, D. Barber, T. Nystul, Cell fate decisions: emerging roles for metabolic signals and cell morphology, EMBO Rep. 18 (2017) 2105–2118, https://doi.org/10.15252/embr.201744816.
[4] P. Gao, W. Pan, N. Li, B. Tang, Fluorescent probes for organelle-targeted bioactive species imaging, Chem. Sci. 10 (2019) 6035–6071, https://doi.org/10.1039/C9SC01652J.
[6] M. Damaghi, J.W. Wojtkowiak, R.J. Gillies, pH sensing and regulation in cancer, Front. Physiol. 4 (2013) 370, https://doi.org/10.3389/fphys.2013.00370.
[7] B. Fang, D. Wang, M. Huang, G. Yu, H. Li, Hypothesis on the relationship between the change in intracellular pH and incidence of sporadic Alzheimer's disease or vascular dementia, Int. J. Neurosci. 120 (2010) 591–595, https://doi.org/10.3109/00207454.2010.505353.
[8] L. Schwartz, S. Peres, M. Jolicoeur, J. da Veiga Moreira, Cancer and Alzheimer's disease: intracellular pH scales the metabolic disorders, Biogerontology 21 (2020) 683–694, https://doi.org/10.1007/s10522-020-09888-6.
[9] D.E. Korenchan, R.R. Flavell, Spatiotemporal pH heterogeneity as a promoter of cancer progression and therapeutic resistance, Cancers 11 (2019), https://doi.org/10.3390/cancers11071026 1026.
[10] S. Eberhard, M. Thomas, Intracellular pH, Circulation 124 (2011) 1806–1807, https://doi.org/10.1161/CIRCULATIONAHA.111.061226.
[11] C.P. Cerrato, K. Künnapuu, Ü. Langel, Cell-penetrating peptides with intracellular organelle targeting, Expert Opin. Drug Deliv. 14 (2017) 245–255, https://doi.org/10.1080/17425247.2016.1213237.
[12] Overview of pH Indicators—Section 20.1 - PL, (n.d.). //www.thermofisher.com/uk/en/home/references/molecular-probes-the-handbook/ph-indicators/overview-of-ph-indicators.html (accessed September 4, 2020).
[13] N.J. Yang, M.J. Hinner, Getting across the cell membrane: An overview for small molecules peptides, and proteins, Methods Mol. Biol. 1266 (2015) 29–53, https://doi.org/10.1007/978-1-4939-2272-7_3.
[14] J.A. Kilgore, N.J. Dolman, M.W. Davidson, A review of reagents for fluorescence microscopy of cellular compartments and structures, Part III: reagents for actin, tubulin, cellular membranes, and whole cell and cytoplasm, Curr. Protoc. Cytom. 67 (2014) 12.32.1–12.32.17, https://doi.org/10.1002/0471142956.cy1232s67.
[15] M. Shamsipur, A. Barati, Z. Nematifar, Fluorescent pH nanosensors: Design strategies and applications, J. Photochem. Photobiol. C Photochem. Rev. 39 (2019) 76–141, https://doi.org/10.1016/j.jphotochemrev.2019.03.001.
[16] J. Han, K. Burgess, Fluorescent indicators for intracellular pH, Chem. Rev. 110 (2010) 2709–2728, https://doi.org/10.1021/cr900249z.
[17] X.-X. Zhang, Z. Wang, X. Yue, Y. Ma, D.O. Kiesewetter, X. Chen, pH-Sensitive fluorescent dyes: Are they really pH-sensitive in cells?, Mol. Pharm. 10 (2013) 1910–1917, https://doi.org/10.1021/mp3006903.
[18] E.A. Specht, E. Braselmann, A.E. Palmer, A critical and comparative review of fluorescent tools for live-cell imaging, Annu. Rev. Physiol. 79 (2017) 93–117, https://doi.org/10.1146/annurev-physiol-022516-034055.
[19] C. Sun, W. Du, B. Wang, B. Dong, B. Wang, Research progress of near-infrared fluorescence probes based on indole heptamethine cyanine dyes in vivo and in vitro, BMC Chem. 14 (2020), https://doi.org/10.1186/s13065-020-00677-321.
[20] W. Zhang, X. Liu, P. Li, W. Zhang, H. Wang, B. Tang, Cellular fluorescence imaging based on resonance energy transfer, TrAC Trends Analyt. Chem. 123 (2020), https://doi.org/10.1016/j.trac.2019.115742 115742.
[21] C. Li, Y. Wang, H. Jiang, X. Wang, Intracellular sensors based on carbonaceous nanomaterials: A review, J. Electrochem. Soc. 167 (2020), https://doi.org/10.1149/1945-7111/ab67a3 037540.
[22] T.T. Hoang Thi, V.D. Cao, T.N.Q. Nguyen, D.T. Hoang, V.C. Ngo, D.H. Nguyen, Functionalized mesoporous silica nanoparticles and biomedical applications, Mater. Sci. Eng. C 99 (2019) 631–656, https://doi.org/10.1016/j.msec.2019.01.129.
[23] V.I. Martynov, A.A. Pakhomov, I.E. Deyev, A.G. Petrenko, Genetically encoded fluorescent indicators for live cell pH imaging, Biochim. et Biophys. Acta (BBA) - General Subjects. 1862 (2018) 2924–2939, https://doi.org/10.1016/j.bbagen.2018.09.013.
[24] M.K. Mahata, H. Bae, K.T. Lee, Upconversion luminescence sensitized pH-nanoprobes, Molecules 22 (2017), https://doi.org/10.3390/molecules22122064 2064.
[25] A. Dembska, P. Bielecka, B. Juskowiak, pH-Sensing fluorescence oligonucleotide probes based on an i-motif scaffold: a review, Anal. Methods. 9 (2017) 6092–6106, https://doi.org/10.1039/C7AY01942D.
[26] C. Wang, T. Zhao, Y. Li, G. Huang, M.A. White, J. Gao, Investigation of endosome and lysosome biology by ultra pH-sensitive nanoprobes, Adv. Drug Deliv. Rev. 113 (2017) 87–96, https://doi.org/10.1016/j.addr.2016.08.014.
[27] Y. Yue, F. Huo, S. Lee, C. Yin, J. Yoon, A review: the trend of progress about pH probes in cell application in recent years, Analyst 142 (2016) 30–41, https://doi.org/10.1039/C6AN01942K.
[28] Y. Jeong, Y.-M. Kook, K. Lee, W.-G. Koh, Metal enhanced fluorescence (MEF) for biosensors: General approaches and a review of recent developments, Biosens. Bioelectronics. 111 (2018) 102–116, https://doi.org/10.1016/j.bios.2018.04.007.
[29] Y. Li, T. Zhao, C. Wang, Z. Lin, G. Huang, B.D. Sumer, J. Gao, Molecular basis of cooperativity in pH-triggered supramolecular self-assembly, Nature Commun. 7 (2016) 13214, https://doi.org/10.1038/ncomms13214.
[30] N.J. Dolman, J.A. Kilgore, M.W. Davidson, A review of reagents for fluorescence microscopy of cellular compartments and structures, part I: BacMam labeling and reagents for vesicular structures, Curr Protoc Cytom. Chapter 12 (2013) Unit 12.30. https://doi.org/10.1002/0471142956.cy1230s65.
[31] X. Ma, Y. Wang, T. Zhao, Y. Li, L.-C. Su, Z. Wang, G. Huang, B.D. Sumer, J. Gao, Ultra-pH-sensitive nanoprobe library with broad pH tunability and fluorescence emissions, J. Am. Chem. Soc. 136 (2014) 11085–11092, https://doi.org/10.1021/ja5053158.
[32] L. Wang, Y. Zhou, Y. Zhang, G. Zhang, C. Zhang, Y. He, C. Dong, S. Shuang, A novel cell-penetrating Janus nanoprobe for ratiometric fluorescence detection of pH in living cells, Talanta 209 (2020), https://doi.org/10.1016/j.talanta.2019.120436 120436.
[33] H. Huang, F. Dong, Y. Tian, Mitochondria-targeted ratiometric fluorescent nanosensor for simultaneous biosensing and imaging of $O_2^{\bullet-}$ and pH in live cells, Anal. Chem. 88 (2016) 12294–12302, https://doi.org/10.1021/acs.analchem.6b03470.
[34] J. Sun, P. Ling, F. Gao, A Mitochondria-targeted ratiometric biosensor for pH monitoring and imaging in living cells with congo-red-functionalized dual-emission semiconducting polymer dots, Anal. Chem. 89 (2017) 11703–11710, https://doi.org/10.1021/acs.analchem.7b03154.
[35] D. Ma, J. Zheng, P. Tang, W. Xu, Z. Qing, S. Yang, J. Li, R. Yang, Quantitative monitoring of hypoxia-induced intracellular acidification in lung tumor cells and tissues using activatable surface-enhanced Raman scattering nanoprobes, Anal. Chem. 88 (2016) 11852–11859, https://doi.org/10.1021/acs.analchem.6b03590.
[36] G. Yang, Q. Zhang, Y. Liang, H. Liu, L.-L. Qu, H. Li, Fluorescence-SERS dual-signal probes for pH sensing in live cells, Coll. Surf. A Physicochem. Eng. Asp. 562 (2019) 289–295, https://doi.org/10.1016/j.colsurfa.2018.11.036.
[37] E. Wiercigroch, E. Stepula, L. Mateuszuk, Y. Zhang, M. Baranska, S. Chlopicki, S. Schlücker, K. Malek, ImmunoSERS microscopy for the detection of smooth muscle cells in atherosclerotic plaques, Biosens. Bioelectronics 133 (2019) 79–85, https://doi.org/10.1016/j.bios.2019.02.068.
[38] J. Langer, D. Jimenez de Aberasturi, J. Aizpurua, R.A. Alvarez-Puebla, B. Auguié, J.J. Baumberg, G.C. Bazan, S.E.J. Bell, A. Boisen, A.G. Brolo, J. Choo, D. Cialla-May, V. Deckert, L. Fabris, K. Faulds, F.J. García de Abajo, R. Goodacre, D. Graham, A.J. Haes, C.L. Haynes, C. Huck, T. Itoh, M. Käll, J. Kneipp, N.A. Kotov, H. Kuang, E.C. Le Ru, H.K. Lee, J.-F. Li, X.Y. Ling, S.A. Maier, T. Mayerhöfer, M. Moskovits, K. Murakoshi, J.-M. Nam, S. Nie, Y. Ozaki, I. Pastoriza-Santos, J. Perez-Juste, J. Popp, A. Pucci, S. Reich, B. Ren, G.C. Schatz, T. Shegai, S. Schlücker, L.-L. Tay, K.G. Thomas, Z.-Q. Tian, R.P. Van Duyne, T. Vo-Dinh, Y. Wang, K.A. Willets, C. Xu, H. Xu, Y. Xu, Y.S. Yamamoto, B. Zhao, L.M. Liz-Marzán, Present and Future of Surface-Enhanced Raman Scattering, ACS Nano. 14 (2020) 28–117, https://doi.org/10.1021/acsnano.9b04224.
[39] P.G. Etchegoin, E.C.L. Ru, Basic Electromagnetic Theory of SERS, in: Surface Enhanced Raman Spectroscopy, John Wiley & Sons, Ltd, 2010: pp. 1–37. https://doi.org/10.1002/9783527632756.ch1.
[40] R. Aroca, S. Rodriguez-Llorente, Surface-enhanced vibrational spectroscopy, J. Mol. Struct. 408–409 (1997) 17–22, https://doi.org/10.1016/S0022-2860(96)09489-6.
[41] A. Kudelski, Raman spectroscopy of surfaces, Surf. Sci. 603 (2009) 1328–1334, https://doi.org/10.1016/j.susc.2008.11.039.

[42] J. Kneipp, H. Kneipp, K. Kneipp, SERS—a single-molecule and nanoscale tool for bioanalytics, Chem. Soc. Rev. 37 (2008) 1052–1060, https://doi.org/10.1039/B708459P.
[43] E.C. Le Ru, M. Meyer, P.G. Etchegoin, Proof of single-molecule sensitivity in surface enhanced Raman scattering (SERS) by means of a two-analyte technique, J. Phys. Chem. B. 110 (2006) 1944–1948, https://doi.org/10.1021/jp054732v.
[44] J. Sun, L. Gong, W. Wang, Z. Gong, D. Wang, M. Fan, Surface-enhanced Raman spectroscopy for on-site analysis: A review of recent developments, Luminescence 35 (2020) 808–820, https://doi.org/10.1002/bio.3796.
[45] W. Wang, J. Wang, Y. Ding, Gold nanoparticle-conjugated nanomedicine: design, construction, and structure–efficacy relationship studies, J. Mater. Chem. B. 8 (2020) 4813–4830, https://doi.org/10.1039/C9TB02924A.
[46] S. Dey, M. Trau, K.M. Koo, Surface-enhanced Raman spectroscopy for cancer immunotherapy applications: opportunities, challenges, and current progress in nanomaterial strategies, Nanomaterials 10 (2020), https://doi.org/10.3390/nano10061145 1145.
[47] N. Akkilic, S. Geschwindner, F. Höök, Single-molecule biosensors: Recent advances and applications, Biosens. Bioelectronics. 151 (2020), https://doi.org/10.1016/j.bios.2019.111944 111944.
[48] M. Fan, G.F.S. Andrade, A.G. Brolo, A review on recent advances in the applications of surface-enhanced Raman scattering in analytical chemistry, Analyt. Chim. Acta 1097 (2020) 1–29, https://doi.org/10.1016/j.aca.2019.11.049.
[49] A. Chakraborty, A. Ghosh, A. Barui, Advances in surface-enhanced Raman spectroscopy for cancer diagnosis and staging, J. Raman Spectros. 51 (2020) 7–36, https://doi.org/10.1002/jrs.5726.
[50] Z. Du, Y. Qi, J. He, D. Zhong, M. Zhou, Recent advances in applications of nanoparticles in SERS in vivo imaging, WIREs Nanomedicine and Nanobiotechnology. n/a (n.d.) e1672. https://doi.org/10.1002/wnan.1672.
[51] J. Noonan, S.M. Asiala, G. Grassia, N. MacRitchie, K. Gracie, J. Carson, M. Moores, M. Girolami, A.C. Bradshaw, T.J. Guzik, G.R. Meehan, H.E. Scales, J.M. Brewer, I. B. McInnes, N. Sattar, K. Faulds, P. Garside, D. Graham, P. Maffia, *In vivo* multiplex molecular imaging of vascular inflammation using surface-enhanced Raman spectroscopy, Theranostics 8 (2018) 6195–6209, https://doi.org/10.7150/thno.28665.
[52] L. Pala, S. Mabbott, K. Faulds, M.A. Bedics, M.R. Detty, D. Graham, Introducing 12 new dyes for use with oligonucleotide functionalised silver nanoparticles for DNA detection with SERS, RSC Adv. 8 (2018) 17685–17693, https://doi.org/10.1039/C8RA01998C.
[53] H. Kearns, R. Goodacre, L.E. Jamieson, D. Graham, K. Faulds, SERS Detection of Multiple Antimicrobial-Resistant Pathogens Using Nanosensors, Anal. Chem. 89 (2017) 12666–12673, https://doi.org/10.1021/acs.analchem.7b02653.
[54] C.L. Zavaleta, B.R. Smith, I. Walton, W. Doering, G. Davis, B. Shojaei, M.J. Natan, S.S. Gambhir, Multiplexed imaging of surface enhanced Raman scattering nanotags in living mice using noninvasive Raman spectroscopy, PNAS 106 (2009) 13511–13516, https://doi.org/10.1073/pnas.0813327106.
[55] A. Jaworska, K. Malek, N. Kachamakova-Trojanowska, S. Chlopicki, M. Baranska, The uptake of gold nanoparticles by endothelial cells studied by surface-enhanced Raman spectroscopy, Biomed. Spectros. Imag. 2 (2013) 183–189, https://doi.org/10.3233/BSI-130047.
[56] K. Malek, A. Jaworska, P. Krala, N. Kachamakova-Trojanowska, M. Baranska, Imaging of macrophages by surface enhanced Raman spectroscopy (SERS), Biomed. Spectros. Imag. 2 (2013) 349–357, https://doi.org/10.3233/BSI-130052.
[57] J. Kneipp, H. Kneipp, B. Wittig, K. Kneipp, Following the dynamics of pH in endosomes of live cells with SERS nanosensors, J. Phys. Chem. C 114 (2010) 7421–7426, https://doi.org/10.1021/jp910034z.
[58] A. Jaworska, T. Wojcik, K. Malek, U. Kwolek, M. Kepczynski, A.A. Ansary, S. Chlopicki, M. Baranska, Rhodamine 6G conjugated to gold nanoparticles as labels for both SERS and fluorescence studies on live endothelial cells, Microchim. Acta. 182 (2015) 119–127, https://doi.org/10.1007/s00604-014-1307-5.
[59] L.E. Jamieson, A. Jaworska, J. Jiang, M. Baranska, D.J. Harrison, C.J. Campbell, Simultaneous intracellular redox potential and pH measurements in live cells using SERS nanosensors, Analyst 140 (2015) 2330–2335, https://doi.org/10.1039/C4AN02365J.
[60] A. Jaworska, L.E. Jamieson, K. Malek, C.J. Campbell, J. Choo, S. Chlopicki, M. Baranska, SERS-based monitoring of the intracellular pH in endothelial cells: the influence of the extracellular environment and tumour necrosis factor-α, Analyst 140 (2015) 2321–2329, https://doi.org/10.1039/C4AN01988A.
[61] S.-S. Li, M. Zhang, J.-H. Wang, F. Yang, B. Kang, J.-J. Xu, H.-Y. Chen, Monitoring the changes of pH in lysosomes during autophagy and apoptosis by plasmon enhanced Raman imaging, Anal. Chem. 91 (2019) 8398–8405, https://doi.org/10.1021/acs.analchem.9b01250.
[62] A. Capocefalo, D. Mammucari, F. Brasili, C. Fasolato, F. Bordi, P. Postorino, F. Domenici, Exploring the potentiality of a SERS-active pH nano-biosensor, Front. Chem. 7 (2019), https://doi.org/10.3389/fchem.2019.00413 413.
[63] L. Bai, X. Wang, K. Zhang, X. Tan, Y. Zhang, W. Xie, Etchable SERS nanosensor for accurate pH and hydrogen peroxide sensing in living cells, Chem. Commun. 55 (2019) 12996–12999, https://doi.org/10.1039/C9CC06485K.
[64] B.T. Scarpitti, A.M. Morrison, M. Buyanova, Z.D. Schultz, Comparison of 4-mercaptobenzoic acid surface-enhanced Raman spectroscopy-based methods for pH determination in cells, Appl. Spectros. 74 (2020) 1423–1432, https://doi.org/10.1177/0003702820950768.
[65] X.-S. Zheng, C. Zong, X. Wang, B. Ren, Cell-penetrating peptide conjugated SERS nanosensor for in situ intracellular pH imaging of single living cells during cell cycle, Anal. Chem. 91 (2019) 8383–8389, https://doi.org/10.1021/acs.analchem.9b01191.
[66] Y. Zhang, D. Jimenez de Aberasturi, M. Henriksen-Lacey, J. Langer, L.M. Liz-Marzán, Live-cell surface-enhanced Raman spectroscopy imaging of intracellular pH: from two dimensions to three dimensions, ACS Sens. 5 (2020) 3194–3206, https://doi.org/10.1021/acssensors.0c01487.
[67] K. Bando, Z. Zhang, D. Graham, K. Faulds, K. Fujita, S. Kawata, Dynamic pH measurements of intracellular pathways using nano-plasmonic assemblies, Analyst 145 (2020) 5768–5775, https://doi.org/10.1039/D0AN00986E.
[68] H. Wei, M.R. Willner, L.C. Marr, P.J. Vikesland, Highly stable SERS pH nanoprobes produced by co-solvent controlled AuNP aggregation, Analyst 141 (2016) 5159–5169, https://doi.org/10.1039/C6AN00650G.
[69] H. Liu, Q. Jiang, J. Pang, Z. Jiang, J. Cao, L. Ji, X. Xia, K. Wang, A multiparameter pH-sensitive nanodevice based on plasmonic nanopores, Adv. Funct. Mater. 28 (2018), https://doi.org/10.1002/adfm.201703847 1703847.
[70] S. Li, Z. Liu, C. Su, H. Chen, X. Fei, Z. Guo, Biological pH sensing based on the environmentally friendly Raman technique through a polyaniline probe, Anal. Bioanal. Chem. 409 (2017) 1387–1394, https://doi.org/10.1007/s00216-016-0063-2.
[71] A. Williams, K.J. Flynn, Z. Xia, P.R. Dunstan, Multivariate spectral analysis of pH SERS probes for improved sensing capabilities, J. Raman Spectros. 47 (2016) 819–827, https://doi.org/10.1002/jrs.4910.
[72] M. García-Algar, D. Tsoutsi, M. Sanles-Sobrido, A. Cabot, V. Izquierdo-Roca, P.R. Gil, Subcellular optical pH nanoscale nensor, ChemistrySelect 2 (2017) 8115–8121, https://doi.org/10.1002/slct.201701087.
[73] Z. Heiner, M. Gühlke, V. Živanović, F. Madzharova, J. Kneipp, Surface-enhanced hyper Raman hyperspectral imaging and probing in animal cells, Nanoscale 9 (2017) 8024–8032, https://doi.org/10.1039/C7NR02762A.
[74] Z. Zhang, K. Bando, K. Mochizuki, A. Taguchi, K. Fujita, S. Kawata, Quantitative evaluation of surface-enhanced Raman scattering nanoparticles for intracellular pH sensing at a single particle level, Anal. Chem. 91 (2019) 3254–3262, https://doi.org/10.1021/acs.analchem.8b03276.
[75] M. Xie, F. Li, P. Gu, F. Wang, Z. Qu, J. Li, L. Wang, X. Zuo, X. Zhang, J. Shen, Gold nanoflower-based surface-enhanced Raman probes for pH mapping of tumor cell microenviroment, Cell Proliferation 52 (2019), https://doi.org/10.1111/cpr.12618 e12618.
[76] S.G. Patel, E.J. Sayers, L. He, R. Narayan, T.L. Williams, E.M. Mills, R.K. Allemann, L.Y.P. Luk, A.T. Jones, Y.-H. Tsai, Cell-penetrating peptide sequence and modification dependent uptake and subcellular distribution of green florescent protein in different cell lines, Sci. Rep. 9 (2019) 6298, https://doi.org/10.1038/s41598-019-42456-8.
[77] R. Luo, Y. Li, Q. Zhou, J. Zheng, D. Ma, P. Tang, S. Yang, Z. Qing, R. Yang, SERS monitoring the dynamics of local pH in lysosome of living cells during photothermal therapy, Analyst 141 (2016) 3224–3227, https://doi.org/10.1039/C6AN00467A.
[78] H. Derakhshankhah, S. Jafari, Cell penetrating peptides: A concise review with emphasis on biomedical applications, Biomed. Pharmacother. 108 (2018) 1090–1096, https://doi.org/10.1016/j.biopha.2018.09.097.
[79] Y. Shen, L. Liang, S. Zhang, D. Huang, R. Deng, J. Zhang, H. Qu, S. Xu, C. Liang, W. Xu, Organelle-targeting gold nanorods for macromolecular profiling of subcellular organelles and enhanced cancer cell killing, ACS Appl. Mater. Interf. 10 (2018) 7910–7918, https://doi.org/10.1021/acsami.8b01320.
[80] Y. Shen, L. Liang, S. Zhang, D. Huang, J. Zhang, S. Xu, C. Liang, W. Xu, Organelle-targeting surface-enhanced Raman scattering (SERS) nanosensors for subcellular pH sensing, Nanoscale 10 (2018) 1622–1630, https://doi.org/10.1039/C7NR08636A.
[81] C.J. Eling, T.W. Price, A.R.L. Marshall, F. Narda Viscomi, P. Robinson, G. Firth, A. M. Adawi, J.-S.G. Bouillard, G.J. Stasiuk, A dual-modal SERS/fluorescence gold nanoparticle probe for mitochondrial imaging, ChemPlusChem 82 (2017) 674–680, https://doi.org/10.1002/cplu.201600593.
[82] K.L. Nowak-Lovato, K.D. Rector, Targeted surface-enhanced Raman scattering nanosensors for whole-cell pH imagery, Appl. Spectrosc. 63 (2009) 387–395, https://doi.org/10.1366/000370209787944406.
[83] K.L. Nowak-Lovato, B.S. Wilson, K.D. Rector, SERS nanosensors that report pH of endocytic compartments during FcεRI transit, Anal. Bioanal. Chem. 398 (2010) 2019–2029, https://doi.org/10.1007/s00216-010-4176-8.
[84] J. Guo, A.S. Rubfiaro, Y. Lai, J. Moscoso, F. Chen, Y. Liu, X. Wang, J. He, Dynamic single-cell intracellular pH sensing using a SERS-active nanopipette, Analyst 145 (2020) 4852–4859, https://doi.org/10.1039/D0AN00838A.
[85] A. Pallaoro, G.B. Braun, N.O. Reich, M. Moskovits, Mapping local pH in live cells using encapsulated fluorescent SERS nanotags, Small 6 (2010) 618–622, https://doi.org/10.1002/smll.200901893.
[86] J. Liu, J. Wen, Z. Zhang, H. Liu, Y. Sun, Voyage inside the cell: Microsystems and nanoengineering for intracellular measurement and manipulation, Microsyst. Nanoeng. 1 (2015), https://doi.org/10.1038/micronano.2015.20 15020.
[87] B. Garcia-Moreno, Adaptations of proteins to cellular and subcellular pH, J. Biol. 8 (2009), https://doi.org/10.1186/jbiol199 98.
[88] A.B. Mukherjee, A.P. Appu, T. Sadhukhan, S. Casey, A. Mondal, Z. Zhang, M.B. Bagh, Emerging new roles of the lysosome and neuronal ceroid lipofuscinoses, Mol. Neurodegeneration 14 (2019), https://doi.org/10.1186/s13024-018-0300-6 4.
[89] R. Shi, L. Huang, X. Duan, G. Sun, G. Yin, R. Wang, J.-J. Zhu, Selective imaging of cancer cells with a pH-activatable lysosome-targeting fluorescent probe, Anal. Chim. Acta. 988 (2017) 66–73, https://doi.org/10.1016/j.aca.2017.07.055.

[90] F.-X. Theillet, A. Binolfi, T. Frembgen-Kesner, K. Hingorani, M. Sarkar, C. Kyne, C. Li, P.B. Crowley, L. Gierasch, G.J. Pielak, A.H. Elcock, A. Gershenson, P. Selenko, Physicochemical properties of cells and their effects on intrinsically disordered proteins (IDPs), Chem. Rev. 114 (2014) 6661–6714, https://doi.org/10.1021/cr400695p.

[91] F.B. Loiselle, J.R. Casey, Measurement of intracellular pH, in: Q. Yan (Ed.), Membrane Transporters in Drug Discovery and Development. Methods in Molecular Biology (Methods and Protocols), 637, Humana Press, 2010.

[92] A. Anemone, L. Consolino, F. Arena, M. Capozza, D.L. Longo, Imaging tumor acidosis: a survey of the available techniques for mapping *in vivo* tumor pH, Cancer Metastasis Rev. 38 (2019) 25–49, https://doi.org/10.1007/s10555-019-09782-9.

[93] https://www.thermofisher.com/pl/en/home/references/molecular-probes-the-handbook/probes-for-organelles/probes-for-lysosomes-peroxisomes-and-yeast-vacuoles.html. (Accessed 01 September 2020).

[94] Q. Wan, S. Chen, W. Shi, L. Li, H. Ma, Lysosomal pH rise during heat shock monitored by a lysosome-targeting near-infrared ratiometric fluorescent probe, Angew. Chem. Int. Ed. 53 (2014) 10916–10920, https://doi.org/10.1002/anie.201405742.

[95] H. Guo, Q. Huang, W. Leng, Y. Zhan, B. Behkam, M.R. Willner, H. Wei, L.C. Marr, P.J. Vikesland, Bromide ion-functionalized nanoprobes for sensitive and reliable pH measurement by surface-enhanced Raman spectroscopy, Analyst 144 (2019) 7326–7335, https://doi.org/10.1039/C9AN01699F.